Three-dimensional heat transfer in the mixture of nanoparticles and micropolar MHD plasma with Hall and ion slip effects

Cite as: AIP Advances **8**, 105109 (2018); https://doi.org/10.1063/1.5050670
Submitted: 02 August 2018 • Accepted: 06 September 2018 • Published Online: 08 October 2018

M. Nawaz, Shafia Rana, Imran Haider Qureshi, et al.

Three-dimensional heat transfer in the mixture of nanoparticles and micropolar MHD plasma with Hall and ion slip effects

M. Nawaz,[1,a] Shafia Rana,[1] Imran Haider Qureshi,[1] and T. Hayat[2,3]
[1]*Department of Applied Mathematics & Statistics, Institute of Space Technology, Islamabad 44000, Pakistan*
[2]*Department of Mathematics, Quaid-I-Azam University, Islamabad 44000, Pakistan*
[3]*NAAM Research Group, Faculty of Science, King Abdul-Aziz University, Jeddah 21589, Saudi Arabia*

(Received 2 August 2018; accepted 6 September 2018; published online 8 October 2018)

This study discusses Hall and ion-slip effects in *3D* heat transfer in micropolar plasma. The solution of modeled hydrodynamic boundary value problems are computed by Galerkin finite element method (GFEM). Simulations for velocity, angular velocity and temperature are carried out. Momentum and thermal boundary thickness are greatly affected by Hall and ion currents. Magnitude of angular velocity has increasing behavior when micropolar parameter increased. In view of the results obtained from the present investigation, it is recommended to use micro-polar plasma like blood and plasma polymers if Joule heating dissipations are required. Micro-rotation due to the solid structure in micropolar increases when vortex viscosity is increased. https://doi.org/10.1063/1.5050670

I. INTRODUCTION

Transfer of heat in many natural and industrial processes is an essential and important mechanism. Different mechanisms involve different modes for transport of heat. However, transport of heat in the processes occurring in fluid flow regimes involves three modes of transport of heat (conduction, convection, radiation). Several strategies are introduced by engineers for the enhancement of heat transfer. These include extension of surfaces exposed to heating/cooling source as in case of heat exchangers, use of fluids which are good conductors of heat and mixture of fluids such that the transfer of heat in the mixture of nano-particles and pure fluid can be enhanced. Besides, these conventional methods, investigators working in the design of thermal systems have introduced the method for the enhancement of heat by the dispersion of nano-particles in fluids. This dispersion of nano-particles causes an increase in the ability to transport of heat in the mixture fluid (mixture of base fluid and nano-particles). Due to which thermal system using mixture of nano-particles and base fluid works in an efficient manner. Due to this significance of the use of nano-fluids in thermal systems, numerous studies both experimental and theoretical are conducted. However, some latest studies are being described here. For instance, Besthapu et al.[1] discussed the impact of thermally stratified nano-fluid by incorporating dissipation effects over an exponentially elongating surface. Ramzan et al.[2] computed optimal solution for problem describing flow of Maxwell nano-fluid by considering the buoyancy effects over a spongy stretching surface. Influence of heat absorption/generation on the flow of Oldroyd-B nano-fluid past over stretching surface investigated analytically by Khan et al.[3] The effect of induction of very small metal particles on the transport of heat in water was studied by Rashid et al.[4] Shermet et al.[5] addresses the influence of

[a]Contact information. Tel.: +92 51 9075478 email: nawaz_d2006@yahoo.com (Dr. Muhammad Nawaz)

Buongiorno's model to natural convection of 3D flow of Newtonian nano-fluid by finite difference procedure. Transmission of mass and heat in nano-fluid flow generated by sheet moving with time dependent and space dependent velocities probed by Qasim et al.[6] and they handled the arising equations by built in BVP solver in MAPLE. Comparative studies of two approaches namely OHAM and FEM for the solution of mixed convection in nano-fluid past a surface moving with variable velocity are analyzed by Seth et al.[7] Das et al.[8] examined the entropy analysis of time dependent magneto-nano-fluid past a convectively moving surface and solve the arising model by shooting scheme.

The mechanism of conducting fluid subject to applied magnetic field exhibits different to the dynamics. The distortions of magnetic lines by fluid flow give raise a change in magnetic flux. Due to the change in magnetic flux, the fluid experience a force called Lorentz force and such flows are called magnetohydrodynamic flows. There are many engineering application, where magnetohydrodynamic flows are encountered. For example, refrigerator, nuclear reactors, MHD accelerators, etc. Despite of complexity in mathematical modeling of MHD flows due to the additional magnetohydrodynamic equations, investigators are intensely paying attention to computation and simulations of magnetohydrodynamic flows because of their application in many engineering and daily life. Here we refer the readers to some latest published work. For example, Khan et al.[9] applied the Runge-Kutta integration procedure to study magnetohydrodynamic effects on transport of mass subject to homogeneous-heterogeneous reactions in Carreau fluid. Hayat et al.[10] investigated the endoscopy, heterogeneous and homogeneous-reactions in MHD Re-Eyring fluid under the peristaltic mechanism with radiative heat transmission. In another exploration, Hayat et al.[11] examined the MHD effects in couple stress fluid flow by considering the Soret and Dufour effects in peristalsis induced flow. Chen et al.[12] gave the Lie-group analysis for viscoelastic MHD flow using Riemann-Liouville fractional derivative approach and computed the solution via Grunwald procedure. Turkyilmazoglu[13] discussed the analytic solution to MHD mixed convection fluid flow generated by a sheet moving in nonlinear manner.

Plasma is an electrically conducting fluid and is composed of charged and ions particles. The moving plasma subject to magnetic field experiences Hall and ion forces which are opposite to the force due to the applied magnetic field. Mathematically speaking, generalized Ohm's law together with conservation laws of magnetohydrodynamic are used to model such MHD flows. Motsa et al.[14] formulated mathematical models in term of boundary value problems for simultaneous effects of Hall and ion-slip currents, chemical reaction during diffusion of mass in the flow regime of micro-polar liquid and solved the governing problems numerically. Joule heating effects due to Hall and ion-slip currents in liquid motion by peristaltic mechanism in a rotating channel is studied by Hayat et al.[15] Hayat et al.[16] considered Hall and slip currents in *3D* flow of second grade fluid and computed the analytic solutions for the obtained problems. Hayat et al.[17] developed mathematical model in the form of a set of boundary value problems describing peristaltic mechanism in the presence of various types of chemical reactions. Analytical study is conducted for mixed convention heat transfer in three-dimensional flow by T. Hayat et al.[18] The double diffusion (mass and temperature diffusions) in the transport of single phase specie during transport of heat in three dimensional motion of second grade fluid is analyzed by Hayat et al.[19] Hayat et al.[20] considered the effects of Hall and ion-slip currents of nano-fluid on peristaltic flow. The effects of Hall and ion-slip currents on three-dimensional thermal changes in Maxwell fluid flow is investigated by Nawaz et al.[21]

Transport of heat in flows is greatly affected by the dissipation of heat phenomenon in electrically conducting fluid subject to magnetic field. Thermal boundary layer thickness is increased due to Joule heating and viscous dissipation. Therefore, it is a major concern of the thermal system designers, to control dissipation of heat in order to make system efficient. Due to this reason, several studies on the viscous dissipation of heat in MHD flows are available. Readers are referred to some most relevant studies given in refs. 22–25. Turkyilmazoglu[26] confirmed the existence of duality of the solutions of boundary value problems characterizing heat transfer in micropolar regime. A comprehensive note on the characteristics of nanofluid was published by Turkyilmazoglu[27] in which the importance of scaling of velocity by similarity variable is highlighted. Turkyilmazoglu[28] derived exact analytic solutions for problems describing mixed convection in MHD micropolar liquid over deformable plate. Turkyilmazoglu[29] investigated Brownian and thermophoresis effects on the transfer of heat and mass

using Buongiorno's model and noted a significant impact of Brownian and thermophoresis effect on wall heat flux.

The electrically conducting fluids in the presence of thermal changes radiate electromagnetic waves in the thermal radiation. The transfer of heat in thermally radiating fluids has different characteristics as compare to the heat transfer in no radiating fluids. To model the heat transfer characteristics in the flow of radiating fluids energy equation is modified using Stefan Boltzmann law. Some important studies discussing thermal radiation using Stefan-Boltzmann law (to energy equation) are mentioned in refs. 30–32.

In view of importance of the enhancement of transport of heat due to the dispersion of nano-particles, study on the effects of *Cu* and *Al*-particles on transfer of heat in the flow of plasma on an elastic sheet moving with power-law velocity is conducted. The modeled boundary value problems are solved numerically using FEM which is a powerful technique and is more liberal as compare to the finite difference method (FDM) and FVM schemes. Therefore, FEM techniques are being utilized extensively by researchers in the field of solid mechanics, computational mechanics, electromagnetic etc. For the implementation of GFEM to CFD problems, readers can be referred to Refs. 33–36 and references therein.

The present work has novelty as no study dealing with the enhancement of heat transfer due to the dispersion of nano-particles in non-Newtonian plasma in the presence of magnetic field while considering Hall and ion slip currents is investigated yet. Present work is a novel addition in the exiting literature. The simulations for MHD modeled boundary value problems are performed through GFEM and observations are displayed both graphically and numerically. This manuscript is divided into four sections. Section one related to the introductions. In section two related to the numerical tool *i.e*. GFEM to solve the arising problem. Result and discussion is given in section three and conclusion made in section four.

A. Colloidal suspension and their rheology

Micro-polar fluid is polar fluids with negligible molecules deformation. Examples of micro-polar fluids are colloidal suspension, polymers in which solid structure are immersed, blood and biological fluids. The rheology of micro-polar fluids is totally different to the rheology of other non-Newtonian fluids. Due to solid structure, micropolar fluid exhibits two types of motions (i) micro-motion (micro-rotation) (ii) macro-motion. To capture both macro and micro-motions, two types of constitutive relationships have been introduced. Hence micro-polar rheology is characterized by the constitutive equations.[1–3]

$$\tau_{ij} = (-p + \lambda V_{k,k})\delta_{ij} + \mu(V_{i,j} + V_{j,i}) + \kappa(V_{j,i} - \varepsilon_{ijk}\omega_k) \tag{1}$$

$$C_{ij} = \alpha\omega_{k,k}\delta_{ij} + \beta\omega_{i,j} + \gamma\omega_{j,i} \tag{2}$$

where p, λ, μ, κ, α, β, γ are the pressure and material parameters satisfy the following constraints

$$\kappa > 0, 3\lambda + \kappa + 2\mu > 0, 2\mu + \kappa > 0, 3\alpha + 2\gamma > 0, -\gamma < \beta < \gamma, \gamma > 0. \tag{3}$$

B. Balance laws for macro- and micro-motions

As there are two types of motions in the flow of micropolar fluids. Therefore, one additional conservation law is needed for the modeling of flow of micropolar fluids. The balance laws[37–39] with constitutive in Eqs. (1)–(3) can be written as

$$\nabla \cdot \mathbf{V} = 0, \tag{4}$$

$$\rho_{nf}\frac{d\mathbf{V}}{dt} = \rho_{nf}(\mathbf{J} \times \mathbf{B}) - \nabla p - (\mu_{nf} + \kappa)\nabla \times (\nabla \times \mathbf{V}) + \kappa(\nabla \times \boldsymbol{\omega}), \tag{5}$$

$$\rho_{nf} j\frac{d\boldsymbol{\omega}}{dt} = (\alpha + \beta + \gamma)\nabla(\nabla \cdot \boldsymbol{\omega}) - \gamma\nabla \times (\nabla \times \boldsymbol{\omega}) + \kappa\nabla \times \mathbf{V} - 2\kappa\boldsymbol{\omega}, \tag{6}$$

$$(\rho c_p)_{nf}\frac{dT}{dt} = k_{nf}[\nabla.(\nabla T) + Q(T - T_\infty)] + \frac{1}{\sigma_{nf}}\mathbf{J} \cdot \mathbf{J}, \tag{7}$$

where **V** is the velocity of the fluid, **J** is the current density, **B** is the magnetic field, ρ is the fluid density, μ is the dynamic viscosity of the fluid, $\boldsymbol{\omega}$ is the micro rotation of the fluid, j is the scalar called the micro-inertia coefficient, c_p is the specific heat, T is temperature of fluid, k is the thermal conductivity, κ is the vortex viscosity coefficient, Q is the heat generation/absorption coefficient and σ is the electrical conductivity.

C. Problem statement

We consider three-dimensional heat transfer in the laminar motion of incompressible micro-polar plasma over a sheet moving with *2D* velocity. The surface is elastic and exposed to constant magnetic field. The temperature of sheet is variable and is function of space coordinates x and y. The convectively heat surface is responsible for the transport of heat in flow regime.

D. Boundary layer equations for micro-polar fluids

Applying boundary layer assumptions, one gets

$$\frac{\partial u}{\partial x}+\frac{\partial v}{\partial y}+\frac{\partial w}{\partial z}=0, \tag{8}$$

$$\rho_{nf}\left(u\frac{\partial u}{\partial x}+v\frac{\partial u}{\partial y}+w\frac{\partial u}{\partial z}\right)=(\mu_{nf}+\kappa)\frac{\partial^2 u}{\partial^2 z}-\kappa\frac{\partial h_2}{\partial z}+\frac{\sigma_{nf}B_0^2 u}{(1+\beta_e\beta_i)^2+\beta_e^2}[\beta_e v-(1+\beta_e\beta_i)u], \tag{9}$$

$$\rho_{nf}\left(u\frac{\partial v}{\partial x}+v\frac{\partial v}{\partial y}+w\frac{\partial v}{\partial z}\right)=(\mu_{nf}+\kappa)\frac{\partial^2 v}{\partial^2 z}-\kappa\frac{\partial h_1}{\partial z}-\frac{\sigma_{nf}B_0^2 u}{(1+\beta_e\beta_i)^2+\beta_e^2}[\beta_e u-(1+\beta_e\beta_i)v], \tag{10}$$

$$\rho_{nf}j\left(u\frac{\partial h_1}{\partial x}+v\frac{\partial h_1}{\partial y}+w\frac{\partial h_1}{\partial z}\right)=\gamma\frac{\partial^2 h_1}{\partial^2 z}-\kappa\left(2h_1+\frac{\partial v}{\partial z}\right), \tag{11}$$

$$\rho_{nf}j\left(u\frac{\partial h_2}{\partial x}+v\frac{\partial h_2}{\partial y}+w\frac{\partial h_2}{\partial z}\right)=\gamma\frac{\partial^2 h_2}{\partial^2 z}-\kappa\left(2h_2+\frac{\partial u}{\partial z}\right), \tag{12}$$

$$\left.\begin{aligned}(\rho c_p)_{nf}\left(u\tfrac{\partial T}{\partial x}+v\tfrac{\partial T}{\partial y}+w\tfrac{\partial T}{\partial z}\right)&=k_{nf}\left(\tfrac{\partial^2 T}{\partial x^2}+\tfrac{\partial^2 T}{\partial y^2}+\tfrac{\partial^2 T}{\partial z^2}\right)+Q(T-T_\infty)\\&+\tfrac{\sigma_{nf}B_0^2}{(1+\beta_e\beta_i)^2+\beta_e^2}[u^2+v^2]\end{aligned}\right\} \tag{13}$$

where $[u, v, w]$ is the velocity vector, $(h_1, h_2, 0)$ are micro-rotation components, j is the micro inertia density, β_e and β_i are the Hall and the ion-slip parameter, $B_\circ$ is the magnitude of the magnetic induction, respectively. Here, the spin gradient viscosity γ is considered to be constant (Rees and Bossom,[25] Rees and Pop[26]). T is the temperature of the fluid, $K=\kappa/\mu_{nf}$ is the material parameter and $j=\nu_f/a$ are the length scale $\gamma=(\mu+\kappa/2)j=\mu(1+K/2)j$. It is important to note that Eqs. (8)–(13) reduce three-dimensional heat transfer in the flow of electrically non-conducting Newtonian fluid with negligible heat generation/absorption when $k=h_1=h_2=\gamma=B_\circ=Q=0$ and $\nu_{nf}=\nu$. This case is discussed by Khan et al.[40] heat transfer in three-dimensional flow induced by sheet moving with nonlinear velocity. Khan et al.[40] also discussed the case of linear stretching elastic surface.

No slip assumption gives boundary conditions which are

$$\left.\begin{aligned}&u=a(x+y),\ v=b(x+y),\ w=0,\ \ h_1=-n\frac{\partial v}{\partial z},\\&h_2=n\frac{\partial u}{\partial z},\ T_w=T_\infty+a(x+y),\ T=T_w\ \text{ as }\ z=0\end{aligned}\right\} \tag{14}$$

$$u=0,\ \ v=0,\ \ w=0,\ \ h_1=h_2=0,\ T\to T_\infty\}\ z\to\infty, \tag{15}$$

where the constants a and b represent the stretching rate, in $x-$ and $y-$ directions having dimensions $(\text{time})^{-1}$ and $n=0,\ 1/2,\ 1$. For $n=0$ is the classic case of strong interaction *i.e* the fluid

particles are unable to rotate at the solid boundary whereas $n = 1/2$ is the case when fluid particles rotate at the solid surface. This case is called weak interactions. For $n = 1$ is the case of turbulent flow which is beyond the scope of this study. These facts are mentioned in several published works.

E. Mathematical model for nano-particles

There are various models (empirical formulas) describing the relationship among physical properties of the base fluid, metallic nano-particles and nanofluid. In this investigation we have use the following model by Das et al.[8]

$$\rho_{nf} = (1-\varphi)\rho_f + \varphi\rho_s, (\rho c_p)_{nf} = (1-\varphi)\left(\rho c_p\right)_f + \varphi\left(\rho c_p\right)_s, \tag{16}$$

$$\sigma_{nf} = \sigma_f\left(1 + \frac{3(\sigma-1)\varphi}{\sigma+2-(\sigma-1)\varphi}\right), \ \sigma = \frac{\sigma_s}{\sigma_f}, \ k_{nf} = \frac{k_s + 2k_f - 2\varphi(k_f - k_s)}{k_s + 2k_f + \varphi(k_f - k_s)}, \tag{17}$$

where φ is the volume fraction. The subscripts f, nf and s stands for fluid, nano-fluid and solid structure (nano-particles). Thermo-physical properties of micro-polar and four types of metallic nano-particles are shown in Table I.

F. Dimensionless procedure

In view of the importance of the results obtained from dimensionless form of conservation equations, the following transformations are introduced

$$\left.\begin{aligned} u = a(x+y)f'(\eta), \ v = b(x+y)g'(\eta), \ w = -(a\nu_{nf})^{\frac{1}{2}}(g+f), \ \theta = \tfrac{T-T_w}{T_w-T_\infty} \\ h_1 = a(\tfrac{a}{\nu_{nf}})^{\frac{1}{2}}(x+y)F(\eta), \ h_2 = a(\tfrac{a}{\nu_{nf}})^{\frac{1}{2}}(x+y)G(\eta), \ \eta = (\tfrac{a}{\nu_{nf}})^{\frac{1}{2}}z \end{aligned}\right\} \tag{18}$$

where ν is the kinematic viscosity. By substituting Eq. (18) in Eqs. (8)–(15), one gets

$$(1+K)f''' - KG' + \frac{\varphi_2 M^2}{(1+\beta_e\beta_i)^2 + \beta_e^2}[\beta_e g' - (1+\beta_e\beta_i)f'] - \varphi_1[f'^2 + g'f' - (f+g)f''] = 0, \tag{19}$$

$$(1+K)g''' + KF' - \frac{\varphi_2 M^2}{(1+\beta_e\beta_i)^2 + \beta_e^2}[\beta_e f' - (1+\beta_e\beta_i)g'] - \varphi_1[g'^2 + g'f' - (f+g)g''] = 0, \tag{20}$$

$$(1+\frac{K}{2})F'' - K[2F + g''] - \varphi_1[(f'+g')F - (f+g)F'] = 0, \tag{21}$$

$$(1+\frac{K}{2})G'' - K[2G - f''] - \varphi_1[(f'+g')G - (f+g)G'] = 0, \tag{22}$$

$$\frac{k_{nf}}{k_f}\theta'' + \beta\mathrm{Pr}\theta + \varphi_2\frac{\mu_{nf}}{\mu_f}\frac{M^2\mathrm{Pr}Ec}{(1+\beta_e\beta_i)^2 + \beta_e^2}[f'^2 + g'^2] - \varphi_3\mathrm{Pr}[f'+g']\theta + \varphi_3\mathrm{Pr}[f+g]\theta' = 0, \tag{23}$$

TABLE I. Different properties of blood and nano-particles.[8]

Physical property	blood/base fluid	*Cu*	*Ag*	Al_2O_3	TiO_2
$\rho/(Kg.m^{-3})$	1060	8933	10500	3970	4250
$c_p/(J\cdot kg^{-1}\cdot K^{-1})$	3770	385	235	765	686.2
$k/(W\cdot m^{-1}\cdot K^{-1})$	0.492	401	429	40	8.9538
φ	0.00	0.05	0.10	0.15	0.20
$\sigma/(s.m^{-1})$	4.3×10^{-5}	59.6×10^{6}	6.6×10^{-7}	35×10^{6}	2.6×10^{6}

and boundary condition becomes

$$\begin{aligned} &g(0)=0,\ f(0)=0,\ g'(0)=\frac{b}{a}=\lambda,\ f'(0)=1,\ F(0)=-\frac{1}{2}ng''(0),\ G(0)=\frac{1}{2}nf''(0),\\ &g'(\infty)=0,\ f'(\infty)=0,\ F(\infty)=0,\ G(\infty)=0,\ \theta(0)=1,\ \theta(\infty)=0 \end{aligned} \tag{24}$$

where λ is the stretching rate parameter.

$$\begin{aligned} \varphi_1=(1-\varphi)^{\frac{5}{2}}(1-\varphi+\varphi\tfrac{\rho_s}{\rho_f}),\ \varphi_2=(1-\varphi)^{\frac{5}{2}}(1+\tfrac{3(\sigma-1)\varphi}{\sigma+2-(\sigma-1)\varphi}),\ \varphi_3=1-\varphi+\tfrac{\varphi(\rho c_p)_s}{(\rho c_p)_f}\\ \beta=\tfrac{Q_0}{a(\rho c_p)_f},\ M^2=\tfrac{\sigma_f B_o^2(1-ct)}{a\rho_f},\ \mathrm{Pr}=\tfrac{\mu_f(c_p)_f}{k_f},\ Ec=\tfrac{(\frac{ax}{1-ct})^2}{(c_p)_f(T_w-T_\infty)}, \end{aligned} \tag{25}$$

are respectively the volumetric expansion rates, the heat absorption/generation coefficient, the Hartmann, the Prandtl and the Eckert numbers. Further, when $M=\beta=0$ *and* $\varphi_2=\varphi_3=1$ Eqs. (19), (20) and (23) reduce to the special case discussed in published work by Khan et al.[40]

II. COMPUTATIONAL PROCEDURE

GFEM is implemented to carry out the simulations for the transport of heat in three-dimensional motion of micro-polar liquid. As a part of procedure, following steps are followed.

A. Domain discretization

The physical domain (after dimensional analysis) is $[0,\infty]$ and is divided into line elements with nodes per elements.

B. Selection of weight and interpolation functions

As there are two nodes per element, therefore, weight and shape functions interpolation functions) are selected in linear form. Further, as suggested by the Galerkin approach, weight functions are taken equal to the interpolation functions. These interpolation functions are defined by $\psi_j=(-1)^{j-1}(\eta_{j+1}-\eta)/(\eta_{j+1}-\eta_j)$, $j=1,\ 2$.

C. Construction of residual equations

Residual equations are defined and are multiplied by weights. The resulting weighted residuals are integrated over a typical element $[\eta_e,\eta_{e+1}]$.

D. Weak form of weighted residuals

The weighted integral residual are integrated over the line element to convert strong form of weighted residual into weak form.

E. Derivation of stiffness coefficients

The dependent unknowns f,g,h,F,G and θ are approximated over a typical element $[\eta_e,\eta_{e+1}]$ by following finite element approximations,[29]

$$h=\sum_{j=1}^{2}\psi_j h_j,\ g=\sum_{j=1}^{2}\psi_j g_j,\ f=\sum_{j=1}^{2}\psi_j f_j,\ F=\sum_{j=1}^{2}\psi_j F_j,\ G=\sum_{j=1}^{2}\psi_j G_j,\ \theta=\sum_{j=1}^{2}\psi_j\theta_j, \tag{26}$$

where f_j, g_j, h_j, F_j, G_j and θ_j are unknown discrete values. ψ_j is the shape function. Using above approximations in weak formulation of weighted residuals, one obtains

$$\begin{aligned} &K_{ij}^{11}=\int_{\eta_e}^{\eta_{e+1}}\psi_i\frac{d\psi_j}{d\eta}d\eta,\ K_{ij}^{13}=-\int_{\eta_e}^{\eta_{e+1}}\psi_i\psi_j d\eta,\ K_{ij}^{12}=0,\ K_{ij}^{14}=0,\ K_{ij}^{15}=0,\\ &K_{ij}^{16}=0,\ K_{ij}^{17}=0,\ K_{ij}^{21}=0,\ K_{ij}^{23}=0,\ K_{ij}^{25}=0,K_{ij}^{26}=0,\ K_{ij}^{27}=0, \end{aligned}$$

$$K_{ij}^{22}=\int_{\eta_e}^{\eta_{e+1}}\psi_i\frac{d\psi_j}{d\eta}d\eta,\ K_{ij}^{24}=-\int_{\eta_e}^{\eta_{e+1}}\psi_i\psi_j d\eta, K_{ij}^{31}=0,\ K_{ij}^{32}=0,\ K_{ij}^{35}=0\,,$$

$$K_{ij}^{36}=\int_{\eta_e}^{\eta_{e+1}}-K\psi_i\frac{d\psi_j}{d\eta}d\eta,\ K_{ij}^{34}=\int_{\eta_e}^{\eta_{e+1}}\frac{\varphi_2M^2}{(1+\beta_e\beta_i)^2+\beta_e^2}\beta_e\psi_i\psi_j d\eta,$$

$$K_{ij}^{37}=0,\ K_{ij}^{33}=\int_{\eta_e}^{\eta_{e+1}}[-(1+K)\frac{d\psi_i}{d\eta}\frac{d\psi_j}{d\eta}-\frac{\varphi_2M^2}{(1+\beta_e\beta_i)^2+\beta_e^2}(1+\beta_e\beta_i)\psi_i\psi_j$$
$$-\varphi_1(\bar{h}+\bar{k})\psi_i\psi_j+\varphi_1(\bar{f}+\bar{g})\psi_i\frac{d\psi_j}{d\eta}]d\eta,$$

$$K_{ij}^{41}=0,\ K_{ij}^{42}=0,\ K_{ij}^{46}=0,\ K_{ij}^{47}=0,\ K_{ij}^{43}=\int_{\eta_e}^{\eta_{e+1}}-\frac{\varphi_2M^2}{(1+\beta_e\beta_i)^2+\beta_e^2}\beta_e\psi_i\psi_j d\eta,$$

$$K_{ij}^{45}=\int_{\eta_e}^{\eta_{e+1}}K\psi_i\frac{d\psi_j}{d\eta}d\eta,\ K_{ij}^{44}=\int_{\eta_e}^{\eta_{e+1}}[-(1+K)\frac{d\psi_i}{d\eta}\frac{d\psi_j}{d\eta}+\varphi_1(\bar{f}+\bar{g})\psi_i\frac{d\psi_j}{d\eta}$$
$$+\frac{\varphi_2M^2}{(1+\beta_e\beta_i)^2+\beta_e^2}(1+\beta_e\beta_i)\psi_i\psi_j-\varphi_1(\bar{h}+\bar{k})\psi_i\psi_j]d\eta,$$

$$K_{ij}^{51}=0,\ K_{ij}^{52}=0,\ K_{ij}^{53}=0,\ K_{ij}^{56}=0,\ K_{ij}^{54}=\int_{\eta_e}^{\eta_{e+1}}-K\psi_i\frac{d\psi_j}{d\eta}d\eta,$$

$$K_{ij}^{57}=0,\ K_{ij}^{55}=\int_{\eta_e}^{\eta_{e+1}}[-(1+\frac{K}{2})\frac{d\psi_i}{d\eta}\frac{d\psi_j}{d\eta}-2K\psi_i\psi_j-\varphi_1(\bar{h}+\bar{k})\psi_i\psi_j+\varphi_1(\bar{f}+\bar{g})\psi_i\frac{d\psi_j}{d\eta}]d\eta,$$

$$K_{ij}^{61}=0,\ K_{ij}^{62}=0,\ K_{ij}^{64}=0,K_{ij}^{67}=0,\ K_{ij}^{65}=0,\ K_{ij}^{63}=\int_{\eta_e}^{\eta_{e+1}}K\psi_i\frac{d\psi_j}{d\eta}d\eta,$$

$$K_{ij}^{66}=\int_{\eta_e}^{\eta_{e+1}}[-(1+\frac{K}{2})\frac{d\psi_i}{d\eta}\frac{d\psi_j}{d\eta}-2K\psi_i\psi_j-\varphi_1(\bar{h}+\bar{k})\psi_i\psi_j+\varphi_1(\bar{f}+\bar{g})\psi_i\frac{d\psi_j}{d\eta}]d\eta,$$

$$K_{ij}^{75}=0,\ K_{ij}^{76}=0,\ K_{ij}^{73}=\int_{\eta_e}^{\eta_{e+1}}\varphi_2\frac{k_f}{k_{nf}}\frac{\mu_{nf}}{\mu_f}\frac{\varphi_2M^2\mathrm{Pr}Ec}{(1+\beta_e\beta_i)^2+\beta_e^2}\bar{h}\psi_i\psi_j d\eta,$$

$$K_{ij}^{71}=0,\ K_{ij}^{72}=0,\ K_{ij}^{74}=\int_{\eta_e}^{\eta_{e+1}}\frac{k_f}{k_{nf}}\frac{\mu_{nf}}{\mu_f}\frac{\varphi_2M^2\mathrm{Pr}Ec}{(1+\beta_e\beta_i)^2+\beta_e^2}\bar{k}\psi_i\psi_j d\eta,$$

$$K_{ij}^{77}=\int_{\eta_e}^{\eta_{e+1}}[-\frac{d\psi_i}{d\eta}\frac{d\psi_j}{d\eta}+\frac{k_f}{k_{nf}}\beta\mathrm{Pr}\psi_i\psi_j+\frac{k_f}{k_{nf}}\varphi_3\mathrm{Pr}(\bar{f}+\bar{g})\psi_i\frac{d\psi_j}{d\eta}-\frac{k_f}{k_{nf}}\varphi_3\mathrm{Pr}(\bar{f}'+\bar{g}')\psi_i\psi_j]d\eta,$$

in which $\bar{f}_i$, $\bar{g}_i$, $\bar{h}_i$, $\bar{F}_i$, $\bar{G}_i$ and $\bar{\theta}_i$ are nodal values computed at the previous iteration.

F. Assembly process

Following the assembly procedure of finite element approach, we get the system of nonlinear equations is given by

$$[K\{\pi\}]\{\pi\}=\{P\},\tag{27}$$

where $[K\{\pi\}]$ is the matrix involving unknown discrete values. The system of algebraic equations is to be solved numerical by an iterative procedure. Here in this study, Picard linearization procedure is used for linearization. Hence

$$[K\{\pi\}^{r-1}]\{\pi\}^r=\{P\}$$

where $\{\pi\}^{r-1}$ are nodal values computed at $(r-1)^{th}$ iteration and $\{\pi\}^r$ are the nodal values being computed at the r^{th} iteration.

G. Computer implementation

The linearized of algebraic equations are solved iteratively. For computational procedure, we developed a computer code on Matlab. Several computational experiments under tolerance 10^{-5} were done to search infinity for η variable. Simulations are carried out in this study reveal that the asymptotic boundary conditions are satisfied when η is equal to 6. So $\eta_{\max} = 6$ is taken as infinity *i.e.* the computational domain is [0, 6].

H. Convergence and error analysis

The error in the simulated results is calculated using $error = \left|\pi^r - \pi^{r-1}\right|$ till the convergence criteria $\max\left|\pi_i^r - \pi_i^{r-1}\right| < \varepsilon = 10^{-5}$ is satisfied.

III. RESULTS AND DISCUSSION

A. Results validation

For simulations for three dimensional magnetohydrodynamic problems (derived from conservation laws, linear momentum, angular momentum and energy conservation and MHD equation), computer code for powerful numerical technique Galerkin finite element method (GFEM) is developed and code is verified by comparing the computed results (for special case) with the results published by Khan et al.[40] This comparison is displayed in Table II and Table III given below.

Further, from numerical experiments, the following useful information is obtained.

B. Observations regarding macro-motion

The macro-motion of nano-plasma is examined under the variation of β_e, β_i, K and behavior of linear velocities is displayed in Figs. 1–8. Hall force is opposite to the magnetic force and reduces the influence of magnetic field on the flow. Hence opposing Lorentz force is reduced by increasing the Hall force. Hence the flow slows down when the Hall force is increased. Therefore, magnetic field causes a significant reduction in momentum boundary layer thickness. During numerical experiments,

TABLE II. The comparison of present results with the results published by Khan et al.[40] when $K = M = 0$ *and* $\varphi_1 = \varphi_2 = 1$.

	$f''(0)$			$g''(0)$		
λ	Shooting	bvp5c	present	Shooting	bvp5c	present
0	-1	-1	-1.0041434	0	0	0
0.5	-1.224745	- 1.224742	-1.226440	-0.612372	- 0.612371	-0.613220
1	-1.414214	-1.414214	-1.4148725	-1.414214	-1.414214	-1.4148725

TABLE III. The comparison of numerical values of present results with the results published in[40] when $M = \beta = 0$ *and* $\varphi_2 = \varphi_3 = 1$.

		$-\theta'(0)$		
Pr	λ	shooting	bvp5c	present
0.7	0	0.793668	0.793668	0.81039863
	0.5	0.972033	0.972029	0.98228616
	1	1.122406	1.122321	1.12913535
1	0	1.000000	0.999990	1.00414345
	0.5	1.224745	1.224742	1.22644094
	1	1.414214	1.414214	1.41487259
7	0	3.072250	3.072251	3.07018018
	0.5	3.762723	3.762724	3.76099940
	1	4.344818	4.344779	4.34284090

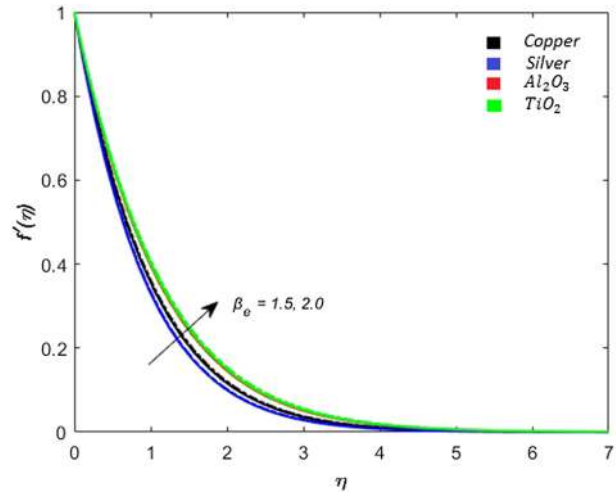

FIG. 1. x-component of velocity curves for β_e with$n = 0$, Pr = 3, $Ec = 2$, $M = 1$, $K = 1$, $\beta_i = 0.9$, $\beta = 0.7$ and $\lambda = 0.5$.

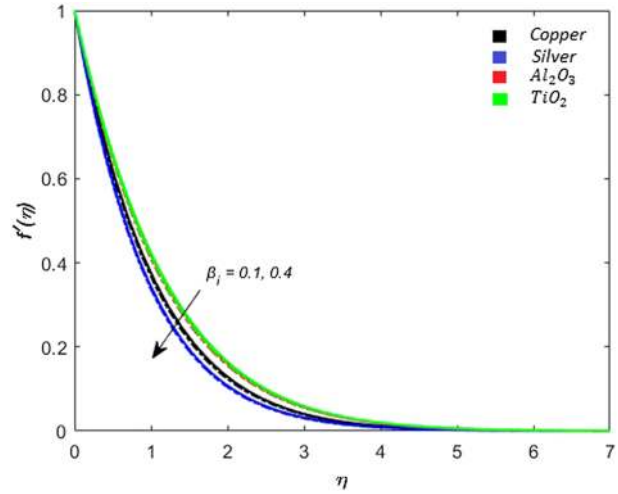

FIG. 2. x-component of velocity curves for β_i with $n = 0$, Pr = 3, $Ec = 2$, $M = 1$, $K = 1$, $\beta_e = 2$, $\beta = 0.7$ and $\lambda = 0.5$.

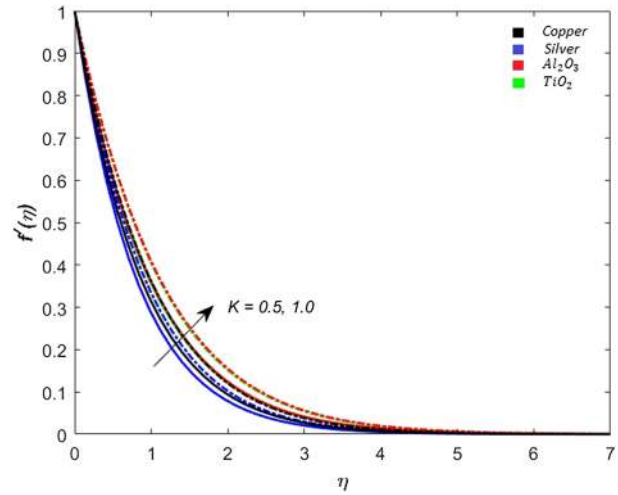

FIG. 3. x-component of velocity curves for K with $n = 0$, Pr = 3, $Ec = 2$, $M = 1$, $\beta_i = 0.9$, $\beta_e = 2$, $\beta = 0.7$ and $\lambda = 0.5$.

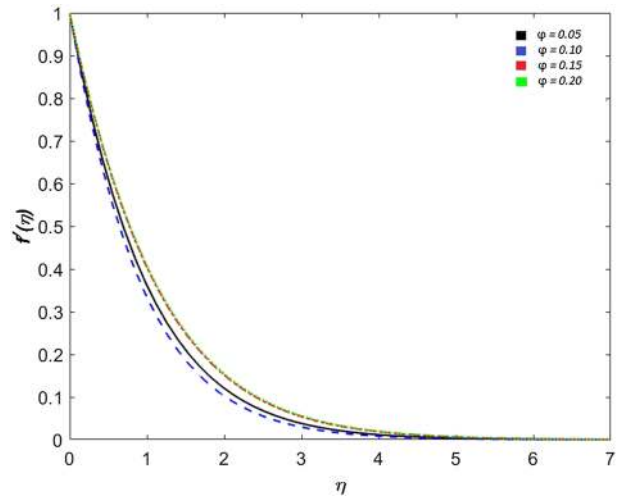

FIG. 4. x-component of velocity curves for φ with $n = 0$, $K = 1$, $Ec = 2$, $M = 1$, $\Pr = 3$, $\beta_i = 0.9$, $\beta_e = 2$, $\beta = 0.7$ and $\lambda = 0.5$.

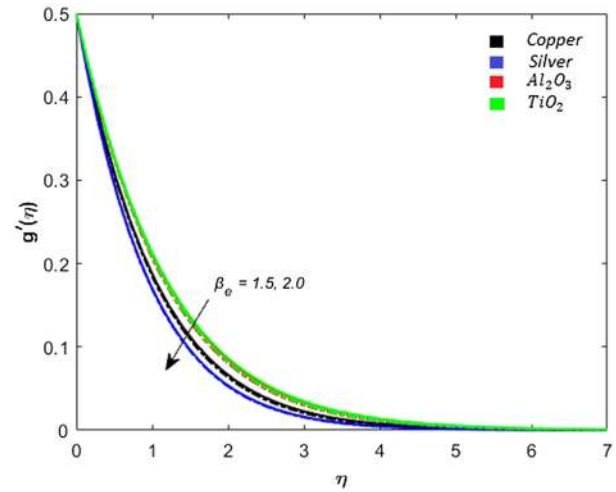

FIG. 5. y-component of velocity curves for β_e with $n = 0$, $\Pr = 3$, $Ec = 2$, $M = 1$, $K = 1$, $\beta_i = 0.9$, $\beta = 0.7$ and $\lambda = 0.5$.

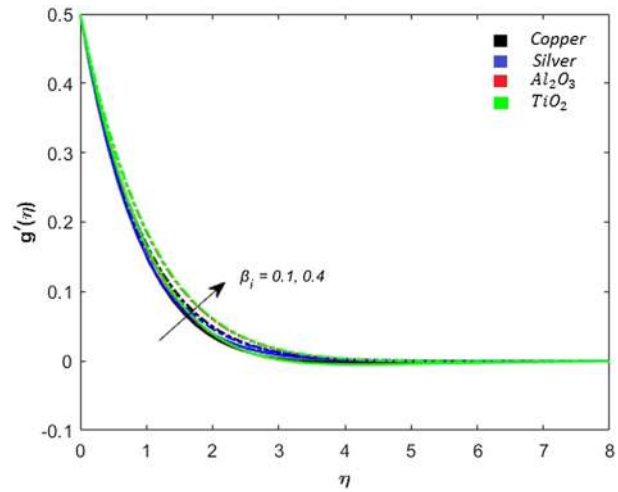

FIG. 6. y-component of velocity curves for β_i with $n = 0$, $\Pr = 3$, $Ec = 2$, $M = 1$, $K = 1$, $\beta_e = 2$, $\beta = 0.7$ and $\lambda = 0.5$.

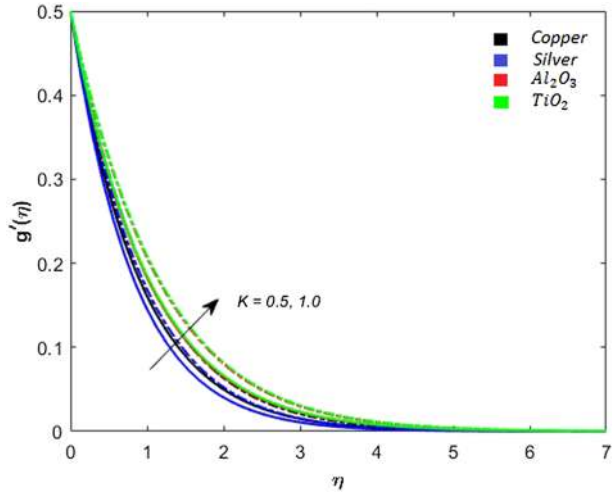

FIG. 7. y-component of velocity curves for K with $n = 0$, $\mathrm{Pr} = 3$, $Ec = 2$, $M = 1$, $\beta_i = 0.9$, $\beta_e = 2$, $\beta = 0.7$ and $\lambda = 0.5$.

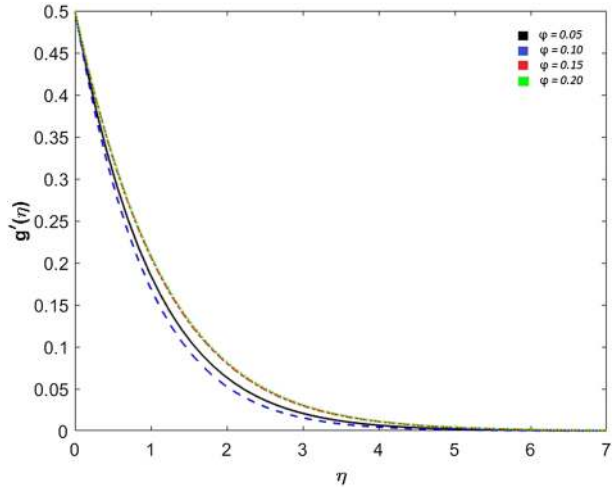

FIG. 8. y-component of velocity curves for φ with $n = 0$, $K = 1$, $Ec = 2$, $M = 1, \mathrm{Pr} = 3$, $\beta_i = 0.9$, $\beta_e = 2$, $\beta = 0.7$ and $\lambda = 0.5$.

simulations are observed and it is noted that velocity of TiO_2 nano-fluid is higher than the velocity of Cu, Ag and Al_2O_3-nano-fluids (see Fig. 1). The comparison of Figs. 1 and 2 represent the effect of ion slip current on the flow in $x-$ direction is quite to the effect of Hall force on the flow in $x-$direction. The behavior of micro-polar parameter on f' (the velocity in $x-$direction) is shown in Fig. 3. This Fig. depict that f' increases when K is increased. Obviously, momentum boundary layer thickness increases by varying K. The effects of dispersion of different type of nano-particles (Cu, Ag, Al_2O_3 and TiO_2) are recorded and displayed in Fig. 4. The influence of β_e, β_i, K and φ on the flow in $y-$direction is studied and displayed in Figs. 5–8. The evident from Figs. 5–8 that flow in $y-$direction is influenced significantly when β_e, β_i and K are varied. The comparison of Figs. 1–4 and 5-8 shows that the effect of β_e, β_i and K on f' are similar to their effects on g'.

C. Observations regarding micro-motion

Micro-rotations are modeled using law of conservation of angular momentum and is made dimensionless using suitable changes of variable. So, $F(\eta)$ and $G(\eta)$ are dimensionless components of angular velocity. Behavior of $F(\eta)$ and $G(\eta)$ under the variation of dimensionless parameters is given in Figs. 9–12. The effects of nano-particles (Cu, Ag, Al_2O_3 and TiO_2) on $F(\eta)$ are represented by Fig. 9. It is notable that the angular velocity (micro-rotation field) for case of Cu-nanoparticles is

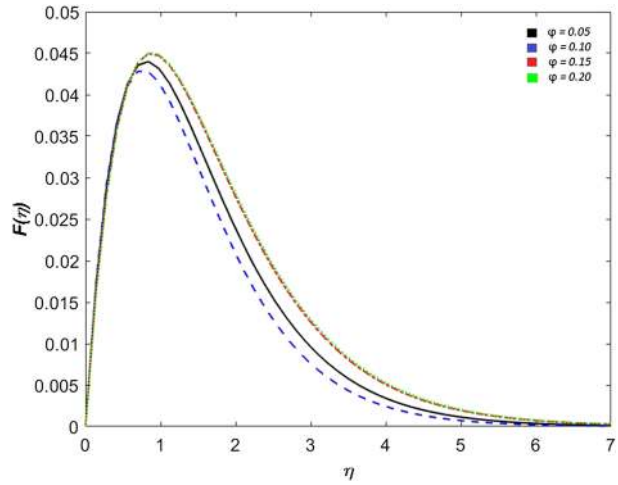

FIG. 9. Effect of φ on $F(\eta)$ when $n = 0$, $K = 1$, $\mathrm{Pr} = 3$, $Ec = 2$, $M = 1$, $\beta_i = 0.9$, $\beta_e = 2$, $\beta = 0.7$ and $\lambda = 0.5$.

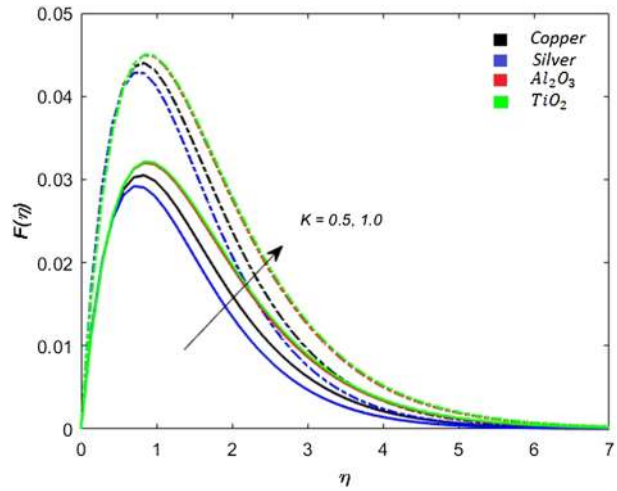

FIG. 10. Effect of K on $F(\eta)$ when $n = 0$, $\mathrm{Pr} = 3$, $Ec = 2$, $M = 1$, $\beta_i = 0.9$, $\beta_e = 2$, $\beta = 0.7$ and $\lambda = 0.5$.

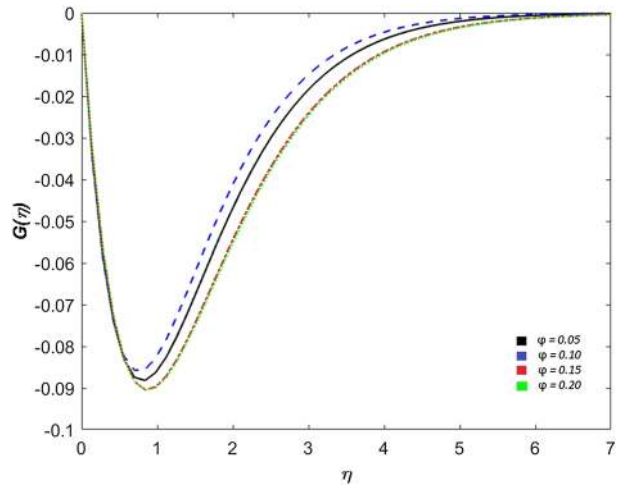

FIG. 11. Effect of φ on $G(\eta)$ when $n = 0$, $K = 1$, $\mathrm{Pr} = 3$, $Ec = 2$, $M = 1$, $\beta_i = 0.9$, $\beta_e = 2$, $\beta = 0.7$ and $\lambda = 0.5$.

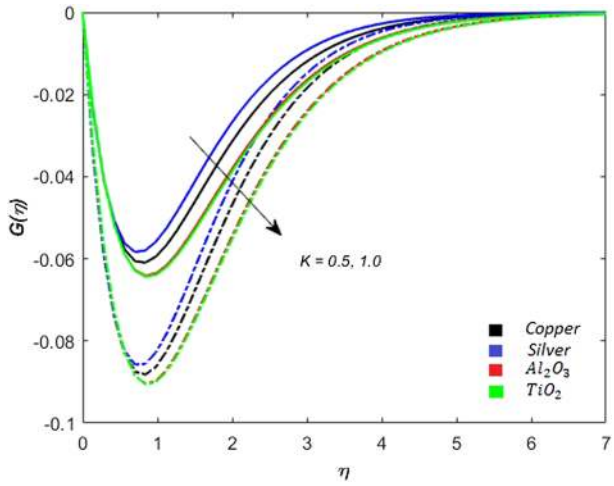

FIG. 12. Effect of K on $G(\eta)$ when $n = 0$, Pr = 3, $Ec = 2$, $M = 1$, $\beta_i = 0.9$, $\beta_e = 2$, $\beta = 0.7$ and $\lambda = 0.5$.

higher than the others nanoparticles (Ag, Al_2O_3 and TiO_2). The effect of micro-polar parameter on $F(\eta)$ is represented in Fig. 10. It is found that the angular velocity is an increasing function of K. It is also noted that nano-fluid containing TiO_2 has higher micro-rotation as compared to Ag, Al_2O_3 and Cu nano fluids. Fig. 11 and 12 depict the similar effects as described in Fig. 9 and 10 respectively.

D. Observations regarding temperature

The temperature curves are displayed in Figs. 13–17. Fig. 13 reveals the behavior of temperature with variation of β_e in case of four types of nano-particles (Cu, Ag, Al_2O_3 and TiO_2). It is obvious from Fig. 13 temperature decreases when Hall force increases. As Hall force has reverse effect on flow in comparison with magnetic field, therefore, it is recommended to use plasma when it is required to reduce Joule heating. Similar observations for temperature are noted when β_i is varied (see Fig. 14). These observations are valid for dispersion of four types of nano-particles. The effect of micro-motions on temperature is displayed in Fig. 15. It is noticed from Fig. 15 that temperature of micro-polar decreases when micro-polar parameter is increased. The thermal boundary layer thickness decreases by increasing K. with an increase in micro-polar parameter. Hence the thermal boundary layer thickness in Newtonian Plasma is higher than the thermal boundary layer thickness in the flow of non-Newtonian fluid. The influence of nano-particles on the transport of heat in micro-polar liquid

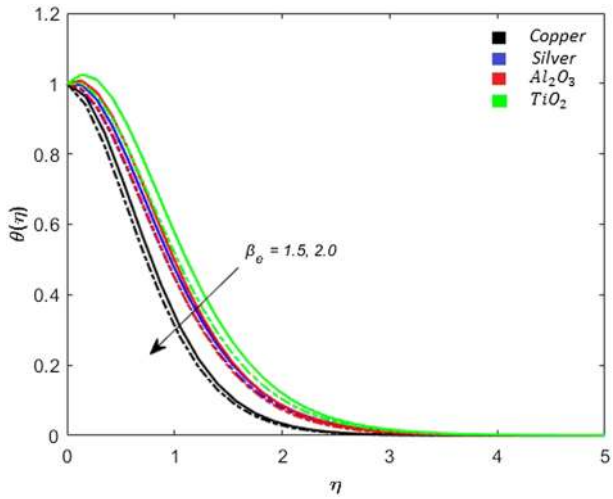

FIG. 13. Temperature distribution when β_e is varied with $n = 0$, Pr = 3, $Ec = 2$, $M = 1$, $K = 1$, $\beta_i = 0.9$, $\beta = 0.7$ and $\lambda = 0.5$.

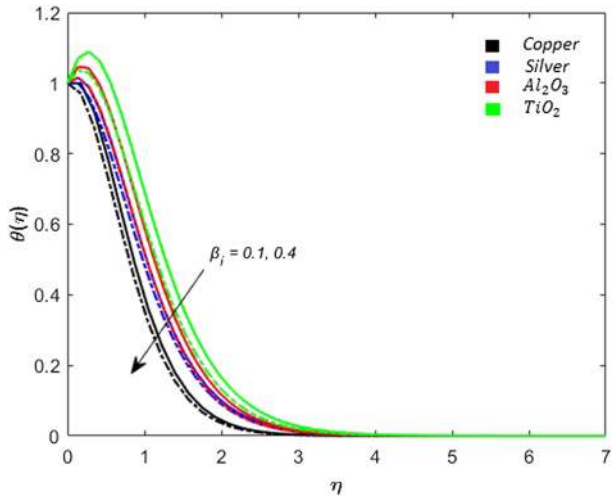

FIG. 14. Temperature distribution when β_i is varied with $n = 0$, Pr = 3, $Ec = 2$, $M = 1$, $K = 1$, $\beta_e = 2$, $\beta = 0.7$ and $\lambda = 0.5$.

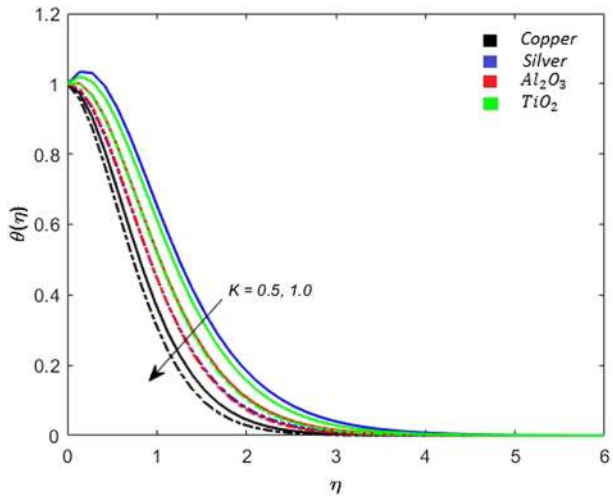

FIG. 15. Temperature curves when K is varied with $n = 0$, Pr = 3, $Ec = 2$, $M = 1$, $\beta_i = 0.9$, $K = 1$, $\beta = 0.7$ and $\lambda = 0.5$.

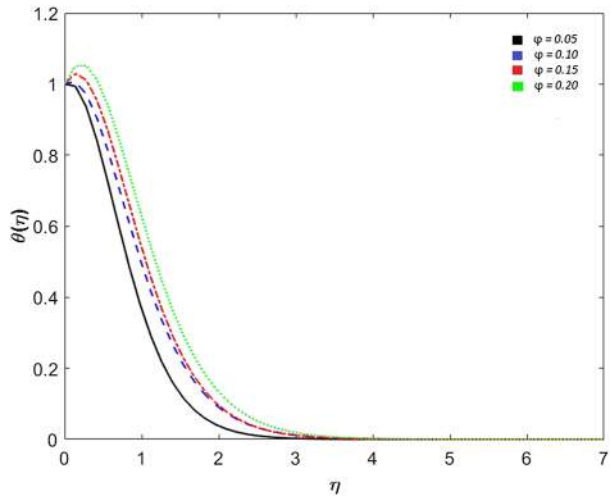

FIG. 16. Temperature distribution for different nano-particles when $n = 0$, $K = 1$, Pr = 3, $Ec = 2$, $M = 1$, $\beta_i = 0.9$, $\beta_e = 2$, $\beta = 0.7$ and $\lambda = 0.5$.

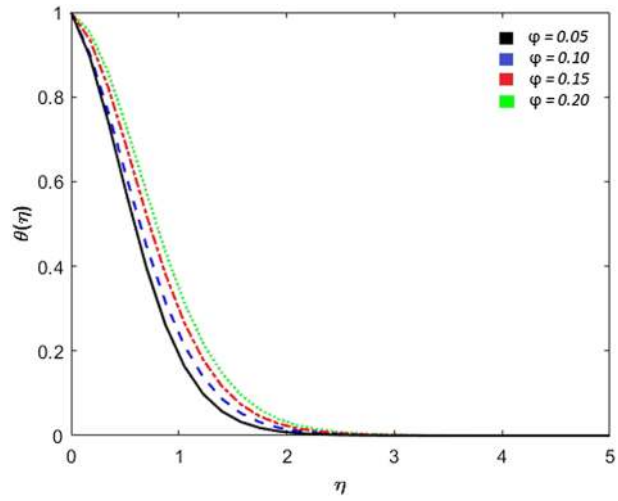

FIG. 17. Temperature distribution for different nano-particles when $n = 0.5$, $K = 1$, $\Pr = 3$, $Ec = 2$, $M = 1$, $\beta_i = 0.9$, $\beta_e = 2$, $\beta = 0.7$ and $\lambda = 0.5$.

is sketched in Fig. 16. It is evident from Fig. 16 that temperature of $Cu-$nano-fluid is greater than the temperature of Ag, Al_2O_3 and TiO_2 nano-fluids. These observations are same for $n = 0$ and $n = 0.5$ in Fig. 17. Thermal boundary layer thickness for Cu-nano-fluid is greater in comparison with the thermal boundary layer thickness for silver, Al_2O_3 and TiO_2-nano-fluids.

IV. CONCLUSION

Three-dimensional transport of heat in the flow of micro-polar liquid subject to four types of nano-particles is modeled. The magnetohydrodynamic boundary value problem with dimensionless form of first law of thermodynamics is solved numerically by using Galerkin finite method (GFEM). After preprocessing, the required formulations for FEM computer code are done. Several numerical experiments are carried for determining the computational domain. The key observations are stated below.

- The force associated with Hall current is favorable forces and cause an enhancement in $x-$component of velocity of the fluid for the case of copper, silver, Al_2O_3 and TiO_2 nano-particles. However, reversal effects for the case of force associated with ion slip currents are seen.
- The flow in x-direction accelerates when K is increased. This increasing trend of primary velocity due to an increase in micro-polar parameter indicates that the primary velocity for Newtonian fluids has less magnitude as compare to the non-Newtonian fluids.
- Secondary velocity decreases when the force associated with Hall current is increased. This shows that the force associated with Hall currents has opposite effect on secondary velocity than its effects on the flow in x-direction.
- The flow in $y-$direction is accelerated when ion slip parameter is increased. It is concluded that force associated with ion slip current is opposite to the direction of force due to the applied magnetics force and is reduced by the force due to ions slip current in $y-$ direction.
- Current (due to Hall and ion-slip) causes a significant reduction in the dissipation of heat due to applied magnetic field. It is also observed that Joules heating dissipation in plasma is less than that in electrically conducting non-plasma fluids.
- Thermal boundary layer thickness in Newtonian fluid greater than that for micro-polar fluids.

ACKNOWLEDGMENTS

This research is carried out under the grant No. 855/Federal/NRPU/R&D/HEC/2016 by HEC, Pakistan.

[1] P. Besthapu, R. U. Haq, S. Bandari, and Q. M. Al-Mdallal, "Mixed convection flow of thermally stratified MHD nanofluid over an exponentially stretching surface with viscous dissipation effect," J. Taiwan Inst. Chem. Eng. **71**, 307–314 (2017).
[2] M. Ramzan, M. Bilal, J. D. Chung, and U. Farooq, "Mixed convective flow of Maxwell nanofluid past a porous vertical stretched surface-an optimal solution," Results Phys. **6**, 1072–1079 (2016).
[3] W. A. Khan, M. Khan, and R. Malik, "Three-dimensional flow of an Oldroyd-B nanofluid towards stretching surface with heat generation/absorption," Plos One **8**, e105108 (2014).
[4] I. Rashid, R. U. Haq, and Q. M. Al-Mdallal, "Aligned magnetic field effects on water based metallic nanoparticles over a stretching sheet with PST and thermal radiation effects," Phys. E **89**, 33–42 (2017).
[5] M. A. Sheremet, I. Pop, and M. M. Rahman, "Three-dimensional natural convection in a porous enclosure filled with a nanofluid using Buongiorno's mathematical model," Int. J. Heat Mass Transfer **82**, 396–405 (2015).
[6] M. Qasim, Z. H. Khan, R. J. Lopez, and W. A. Khan, "Heat and mass transfer in nanofluid thin film over an unsteady stretching sheet using Buongiorno's model," Eur. Phys. J. Plus **131** (2016).
[7] G. S. Seth, M. K. Mishra1, and R. Tripathi, "Modeling and analysis of mixed convection stagnation point flow of nanofluid towards a stretching surface: OHAM and FEM approach," Comp. Appl. Math (2017).
[8] S. Das, S. Chakrabortyi, R. N. Jana, and O. D. Makinde, "Entropy analysis of unsteady magneto-nanofluid flow past accelerating stretching sheet with convective boundary condition," Appl. Math. Mech. **36**, 1593–1610 (2015).
[9] I. Khan, S. Ullah, M. Y. Malik, and A. Hussain, "Numerical analysis of MHD carreau fluid flow over a stretching cylinder with homogenous-heterogeneous reactions," **9**, 1141–1147 (2018).
[10] T. Hayat, J. Akram, A. Alsaedi, and H. Zahir, "Endoscopy and homogeneous-heterogeneous reactions in MHD radiative peristaltic activity of re-eyring fluid," Results Phys. **8**, 481–488 (2018).
[11] T. Hayat, S. Asghar, A. Tanveer, and A. Alsaedi, "Chemical reaction in peristaltic motion of MHD couple stress fluid in channel with Soret and Dufour effects," Results Phys. **10**, 69–80 (2018).
[12] X. Chen, Y. Ye, X. Zhang, and L. Zheng, "Lie-group similarity solution and analysis for fractional viscoelastic MHD fluid over a stretching sheet," Comp. Math. Appl. **8**, 3002–3011 (2018).
[13] M. Turkyilmazoglu, "Analytical solutions to mixed convection MHD fluid flow induced by a nonlinearly deforming permeable surface," Commun. Nonlinear Sci. Numer. Simul. **63**, 373–379 (2018).
[14] S. Motsa and S. Shateyi, "The effects of chemical reaction, Hall and ion-slip currents on MHD micropolar fluid flow with thermal diffusivity using a novel numerical technical," J. App. Math. **9**, 1–30 (2012).
[15] T. Hayat, H. Zahir, A. Alsaedi, and B. Ahmad, "Hall current and Joule heating effects on peristaltic flow of viscous fluid in a rotating channel with convective boundary conditions," Results Phys. 2831–2836 (2017).
[16] T. Hayat and M. Nawaz, "Hall and ion-slip effects on three-dimensional flow of a second grade fluid," Int. J. Numer. Meth. Fluids **7**, 2831–2836 (2017).
[17] T. Hayat, A. Bibi, H. Yasmin, and B. Ahmad, "Simultaneous effects of Hall current and homogeneous/heterogeneous reactions on peristalsis," J. Taiwan Inst. Chem. Eng. **58**, 28–38 (2016).
[18] T. Hayat, M. Awais, M. Nawaz, S. Iram, and A. Saedi, "Mixed convection three-dimensional flow with Hall and ion-slip effects," Int. J. Nonlinear Sci. Number. Simul. **14**, 167–177 (2013).
[19] T. Hayat and M. Nawaz, "Soret and Dufour effects on the mixed convection flow of a second grade fluid subject to Hall and ion-slip current," Int. J. Num. Method's fluids **66**, 1073–1099 (2011).
[20] T. Hayat, M. Shafique, A. Tanveer, and A. Alsaedi, "Hall and ion slip effects on peristaltic flow of Jeffery nanofluid with Joule heating," J. Mag, Mag. Mat. **407**, 51–59 (2016).
[21] M. Nawaz, T. Hayat, and A. Alsaedi, "Mixed convection three-dimensional Maxwell fluid flow in the presence of Hall and ion-slip effects," J. Heat Trans. **135**, 1–8 (2013).
[22] A. K. Pandey and M. Kumar, "Effect of viscous dissipation and suction/injection on MHD nanofluid flow over a wedge with porous medium and slip," Alex. Eng. J. **55**, 3115–3123 (2016).
[23] Y. Shagaiy, D. Zainal, A. Aziza, Z. Ismail, and F. Salah, "Double stratification effects on unsteady electrical MHD mixed convection flow of nanofluid with viscous dissipation and Joule heating," J. Appl. Res. Tech. **15**, 464–476 (2017).
[24] E. Osalusi, J. Side, R. Harris, and B. Johnston, "On the effectiveness of viscous dissipation and Joule heating on steady MHD flow and heat transfer of a Bingham fluid over a porous rotating disk in the presence of Hall and ion-slip currents," Int. Comm. Heat Mass Transf. **34**, 1030–1040 (2007).
[25] E. Osalusi, J. Side, R. Harris, and P. Clark, "The effects of Ohmic heating and viscous dissipation on unsteady MHD and slip flow on a rotating cone in a rotating fluid with variable properties in the presence of Hall and ion-slip currents," Int. Comm. Heat Mass Transf. **35**, 413–429 (2008).
[26] M. Turkyilmazoglu, "A note on micropolar fluid flow and heat transfer over a porous shrinking sheet," Int. J. of Heat and Mass Transfer **72**, 388–391 (2014).
[27] M. Turkyilmazoglu, "A Note on the correspondence between certain nanofluid flows and standard fluid flows," J. of Heat Transfer **137**, 024501–024503 (2015).
[28] M. Turkyilmazoglu, "Mixed convection flow of magnetohydrodynamic micropolar fluid due to a porous heated/cooled deformable plate: Exact solutions," Int. J. of Heat and Mass Transfer **106**, 127–134 (2016).
[29] M. Turkyilmazoglu, "Buongiorno's model in a nanofluid filled asymmetric channel fulfilling zero net particle flux at the walls," Int. J. of Heat and Mass Transfer **126**, 974–979 (2018).
[30] T. Hayat, A. Shafiq, and A. Alseadi, "Effect of joule heating and thermal radiation in the flow of third grade fluid over radiative surface," PLOS One **9**(1), 1–12 (2014).
[31] T. Hayat, M. Awais, A. Alsaedi, and A. Safdar, "On computations for thermal radiation in MHD channel flow with heat and mass transfer," PLOS One **9**(1), 1371–1383 (2014).
[32] T. Hayat and M. Qasim, "Radiation and mass transfer effects on the magnetohydrodynamic unsteady mixed convection flow of second grade fluid over a vertical stretching sheet," Int. J. Num. Meth. Fluid **66**, 820–832 (2011).
[33] M. Nawaz and T. Zubair, "Finite element study of three dimensional radiative nano-plasma flow subject to Hall and ion slip currents," Results in Physics **7**, 4111–4122 (2017).

[34] A. Bejan, "Entropy generation minimization, the new thermodynamics of finite-size devices and finite-time processes," J. Appl. Phys. **79**, 1191–1218 (1996).
[35] J. N. Reddy, *An introduction to the finite element method* (McGraw-Hill, 1984).
[36] J. N. Reddy, *An introduction to the nonlinear finite element analysis* (Oxford University Press, 2005).
[37] A. Kucaba-Pietal, "Microchannel flow modelling with the micropolar fluid theory," The Bulletin of the Polish Academy of Sciences, Technical Sciences **54**(3), 209–214 (2004).
[38] A. C. Eringen, "Theory of micropolar fluids," J. of Math. and Mech. **16**(1), 1–16 (1966).
[39] K. A. Kline and S. J. Allen, "Non-steady flows of fluids with microstructure," Phy. of Fluids **13**, 263–283 (1970).
[40] J. A. Khan, M. Mustafa, T. Hayat, and A. Alsaedi, "On three-dimensional flow and heat transfer over a non-linearly stretching sheet: Analytical and numerical solutions," PLOS ONE **9**(9), e107287 (2014).